ELSEVIER



# Surface ligands engineering of semiconductor quantum dots for chemosensory and biological applications

**Jie Zhou[1], Yun Liu[1], Jian Tang[1] and Weihua Tang[1,2,*]**

[1] College of Chemical Engineering, Nanjing University of Science and Technology, Nanjing 210094, People's Republic of China
[2] State Key Laboratory of Organic-Inorganic Composites, Beijing University of Chemical Technology, Beijing 100029, People's Republic of China

**Featuring size-tunable electrical and optical properties, semiconductor quantum dots (QDs) are appealing intensive interests in developing ingenious luminescent materials for chemosensory and biological applications. The surface modification of QDs with functional ligands not only fine-tunes the physiochemical properties and fluorescence emission behaviors, but also induces the designated interplay between analytes and probes for special determination. In this review, the fundamental principles guiding the rational design of high-efficiency luminescent sensors with surface engineering are overviewed. The state-of-the-art applications of QDs-based probes are highlighted for the sensing of molecular substrates and ionic species as well as various biological applications, with the inherent recognition mechanisms elaborated for representative cases. The challenge and future research direction in this emerging and promising research field are also discussed.**

## Introduction

Semiconductor quantum dots (QDs), commonly referring to II–VI, III–V, and IV–VI binary and their alloyed nanocrystals (1–10 nm), have emerged as an important library of luminescent materials with unique optical, electrical and physical properties [1]. By virtue of the three-dimensional confinement of excited charge carriers within them, QDs demonstrate characteristic size-controlled fluorescent emission. Compared to organic fluorophores, broad emission spectra covering from 450 to 1500 nm can be gained by tailoring their size, shape and composition [2]. Concurrently, their broad absorbance bands allow the photoexcitation of QDs of different sizes or compositions by a single wavelength, making them particularly attractive for multiplex optical sensing [3]. The high resistance ability to photobleaching also enables them serviceable for long-term in vitro and in vivo imaging [4–6]. The bright and potential applications of QDs extremely depend on the structure and properties of nanoscale interfaces.

Surface ligands that possess an anchoring headgroup and end functionalities are an essential component for QDs synthesis, processing and applications. The binding behavior and functional tail of ligands can well-tune the dispersibility in solution and the inherent size-dependent emission [7]. The ligands can play as efficient moderators for the exciton relaxation by affecting the phonon-assisted intraband relaxation, Auger recombination or energy transfer to ligand vibrations in QDs [8]. The photoluminescence quantum yield (PLQY) of QDs is greatly determined by the competitiveness of radiative recombination of band-edge excitons with the electron or hole-trapping processes. The use of σ-donating ligands (e.g. alkylamines) usually can enhance the PLQY of CdSe QDs up to 50% due to the effective passivation for electron traps, thus resulting in weakened non-radiative recombination of excitons [9]. Thiolates are both σ- and π-donating ligands that can effectively passivate electron traps but introduce hole traps. Their increased or decreased effect on PLQY of QDs is therefore complicated, relying on the initial state of QD surface, the adsorption number of thiolates per QD as well as the position of valence band edge of QD [10,11]. The surface ligands thus must be careful screened to control the fluorescence emissions.

An emerging trend with QDs is their use as scaffolds to assemble multiple energy transfer pathways. The nature of the interplay between QDs and surface ligands allows the electronic coupling process such as electron transfer (ET) [12] and fluorescence

*Corresponding author: Tang, W. (whtang@mail.njust.edu.cn)

 http://dx.doi.org/10.1016/j.mattod.2017.02.006

resonance energy transfer (FRET) [13]. In an ET process, the conduction band electrons of QDs move to the conjugated acceptor with lower LUMO energy level, accompanied with a consequent fluorescence quenching. Conversely, the depletion of valence band holes occurs in the presence of electron donor molecules possessing a higher HOMO level energy than the valence band potential. The FRET process proceeds in a dipole-dipole mechanism requiring close proximity of donors and acceptors (up to about twice the Förster distance) as well as finite overlapping between the donor emission and acceptor absorption spectra. This non-radiative transfer of excitation energy can enhance the surface acceptor emission, along with QD emission loss. The QDs emission can be quenched by the use of non-fluorescent acceptor. The ligands with end functionalities decoration afford the interaction possibility for loading donor or acceptor molecules. It is thus impelling intense efforts devoted for surface ligands engineering of QDs for chemosensory and biological sensing [14–16].

Even though a number reviews have been published on the syntheses [17,18], molecular ligands-controlled sensing [15] and bioconjugation strategies [19,20] for QDs, an up-to-date review focusing on the surface ligands engineering of QDs specially for the purpose of aqueous recognition and biological applications is highly demanding. We have organized the review from the role of surface ligands for QDs to the ligands option and functionalization tailoring end applications. Specially, the representative sensing cases in aqueous or biological medium are all presented in recent five years to elucidate the importance of surface chemistry. The proposed sensing mechanisms are also discussed in these cases. Finally, a short outlook on the limitations and prospects of QD-based sensors is provided.

## The role of surface ligands

The ligands engineering on the CDs surface is commonly performed in solution adopting either ''in-synthesis'' or ''post-synthesis'' strategies. In the wet-chemical synthesis process, the influence of ligands on monomers activities is considered more significant in the nucleation stage, which may turn to simultaneously affect the monomers activities and nanocrystals in the further growth. Therefore, not only the size and size distribution but also the shape of QDs can be controlled by ligands types and concentrations [21]. Weiss's group also demonstrated the tuned composition of CdSe QDs surface using 90% TOPO, wherein the ratio of Cd to Se varied from 1.2:1 ($R \geq 3.3$ nm) to 6.5:1 ($R = 1.9$ nm) driven by the $Cd^{2+}$-alkylphosphonate complexes [22]. Furthermore, with an appropriate choice of capping ligands, it was possible to precisely switch the structure between zinc blende and wurtzite for CdSe QDs [23].

Surface ligands enable control over the stability of QDs dispersions in polar or nonpolar solvents via the steric and electrostatic mechanisms. The oleophilic ligands featuring a hydrocarbon tail (see Fig. 1) can afford QDs with superior spectroscopic features and intrinsic solubility in nonpolar solvents. These ligands commonly refer to organic molecules such as trioctylphosphine/trioctylphosphine oxide (TOP/TOPO), long-chain alkylamines and alkylthiols [24]. For the end applications involved in aqueous or biological medium, the water dispersibility of QDs is strongly recommended. The class of organic molecules with hydrophilic tails (e.g. thiolate alcohols, thiolate acids and thiolate siloxane acids as hydrophilic

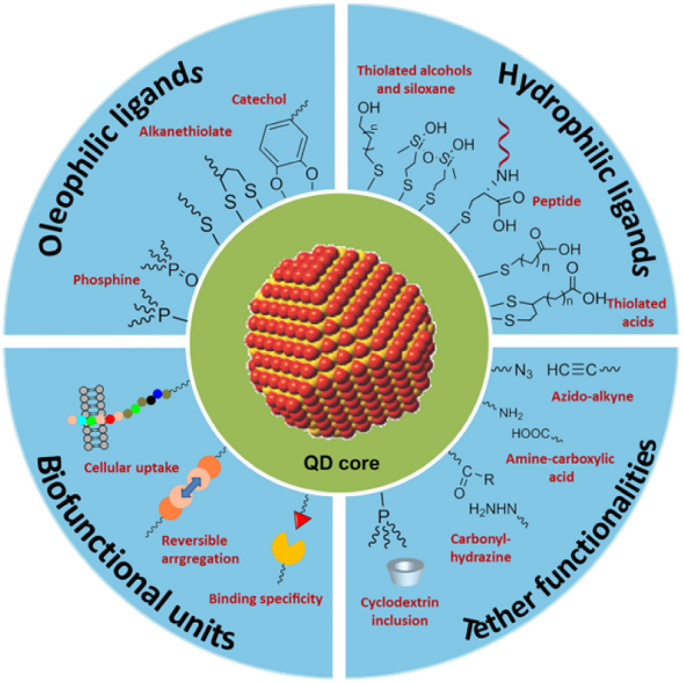


**FIGURE 1**

Surface engineering strategies of QDs for end applications: (a) capping layers using oleophilic ligands, (b) water-soluble surface layers using hydrophilic ligands, (c) versatile tether functionalities via selective reactions or interactions, (d) biofunctionalities for targeting or therapeutic applications.

ligands in Fig. 1) are adopted as ligands to produce aqueous QDs in either direct wet-chemical synthesis [25,26] or post-synthetic ligands exchange [27]. The ligands employed are supposed to guarantee the phase transfer efficiency and retain the PLQY of oleophilic QDs. In this aspect, the ligands possessing more than one coordinating unit can afford QDs extraordinary stability with varied pH medium and the lengthened storage time. These emerging ligands appended hydrophilic polymers or zwitterions are helpful in the bioanalysis [28]. Recently, the ligands pioneered by Talapin's group are inorganic ligands including chalcogenidometallates, metal-free chalcogenides, halides, pseudohalides, oxoanions/polyoxometallates and halometallates for electronic, optoelectronic, and thermoelectric applications [29–32]. However, to meet the motif of this review, we will exclude this kind of ligands in the following discussions.

Another highlighted role of surface ligands is to provide a platform for anchoring functionalities. The bare QDs are endowed with the sensing ability aroused from the physical or chemical interactions on surface, while only limited molecules or ions can directly react with QDs surface. The functionalities at the outer shell is thus of vital importance to improve the interaction possibility and selectivity. To further fine-tune the versatility of QDs functionality, covalent conjugation or non-covalent interaction of secondary molecule layer alongside or onto the first ligand layers are post-synthetically performed (tethered functionalities in Fig. 1). The surface chemistry can be implemented via the amide linkage formation [33], azide-alkyne 'click chemistry' [34,35] and aldehyde-hydrazine reactions [36], etc. It is noteworthy that the concept of bioorthogonality derived from click chemistry has actuated selective label or conjugation of target molecules via a highly chemoselective way on QDs surface [37,38]. Besides, the

utilization of 'host–guest' inclusion complexation derived from supramolecules chemistry (e.g. long alkyl chain embed in hydrophobic cavity of cyclodextrins) is a representative non-covalent strategies [39]. Likewise, the amphiphilic polymers can directly encapsulate QDs based on hydrophobic effects with hydrocarbon of pristine ligands [40,41]. In such cases, amphiphilic polymers act as both surface stabilizer and functionalities scaffolds. The biocompatibility of QDs-based probes is an essential prerequisite for the use of in targeting, therapy as well as in vitro and in vivo sensing. Surface modifications have to offer an active site to build a specific label by taking account of possible biofunctionalization.

## Ligands-driven molecular sensing

QDs are appealing platforms for developing luminescent sensors by chemical modification with recognition units. Supramolecular chemistry has been paid much attention in building functional materials due to the unique feature to form reversible non-covalent interactions between macrocyclic hosts and guests [42]. The supramolecules engaged on QDs surface cover pillararenes [43], calixarenes [44], cucurbiturils [45] and cyclodextrins (CDs). The former three supramolecules can adsorb on QDs surface by host–guest inclusion complexation or electrostatic interactions. The encapsulation of targeted molecules in the cavity enables ligands desorb from QDs surface and switch the fluorescence emission. The reversible and weak interactions might lower the stability compared to covalent bridge. Compared to CDs, the adoption of them is lack due to their more complex synthesis and functionalization. Accordingly, this section is going to update the CDs-capped QDs sensors for organic low-molecular-weight substrates. The sensing of small molecules using other ligands modified QDs probes can be found in other reviews [3,15].

### *The sensing of achiral molecules*

The commonly used CDs comprise 6–8D-glucopyranose units, featuring unique configuration with a hydrophilic rim and a hydrophobic cavity. CDs essentially present two prominent selectivities: internal selectivity (encapsulate guest molecules governed by the cavity size) and external selectivity (dependent on the functional groups on the rims) [46]. Table 1 summarizes the representative QDs-fluorescent sensors for achiral and chiral molecules.

The non-covalently adsorption to QDs surface undergoes direct encapsulate the long alkyl chain of oleophillic ligands. For instance, the fluorescence emission of CdSe/ZnS QDs was effectively quenched when the outer ketoprofen moiety was non-covalently embedded into CD-Py cavity (Fig. 2A). The fluorescence emission can be recovered by stripping CDs using 7 analytes with stronger capture ability (phenol, benzophenone and analogy, indole, 7-methylindole and 1-adamantanecarboxylic acid) [47]. In the case of CD covalently linked CdTe QDs by reacting with boric acid (Fig. 2B), the determination for amantadine was implemented by shutting off the FRET path between QDs and Rhodamine B [48]. Interestingly, enhanced PL intensity of S-β-CD and MSA stabilized CdTe QDs was observed upon the addition of acetylsalicylic acid, since its maximum absorption (~300 nm) coincided with the excitation wavelength of QDs and carboxylic moieties provoked the stability of QDs [49]. Besides, the sensing assay for malachite green [50], ascorbic acid [51] and vanillin [39] was also reported based on CD modified QDs.

The well-designed optical sensors can be used to discriminate isomers which only exhibit slight difference in structures. Chen et al. [52] immobilized Ts-β-CD onto CdTe QDs surface by reacting with (3-aminopropyl)triethoxysilane. The as-obtained aqueous

**TABLE 1**

**Representative CDs-driven molecular recognition of QD-based probes.**

| Molecules | Ligands | QDs | Proposed mechanisms | Ref. |
|---|---|---|---|---|
| **Achiral molecular sensing** | | | | |
| 7 analytes | CD-Py | CdSe/ZnS | The exfoliation of CD complexes with analytes leads to recovered fluorescence | [47] |
| Amantadine | β-CD | CdTe | The formed complexes of amantadine shut off the FRET path of CD with Rhodamine B | [48] |
| Acetylsalicylic acid and its metabolites | S-β-CD, MSA | CdTe | The absorption wavelength of analytes can excite QDs and carboxylic moieties on QDs surface and provoke the stability, leading to enhanced fluorescence | [49] |
| Malachite green | PM-β-CD | CdTe | The formed inclusion complex of PM-β-CD and MG leads to charge transfer-induced quenching | [50] |
| Ascorbic acid | β-CD | CdSe/ZnS | Fluorescence quenching originates from the dehydroascorbic acid induced charge transfer | [51] |
| Vanillin | β-CD | CdSe/ZnS | Fluorescence quenching due to the interaction between vanillin and CD-CdSe/ZnS complex | [39] |
| *o,p*′-DDT, *p,p*′-DDT | Ts-β-CD | CdTe | Different fluorescence quenching behavior due to different association capacity | [52] |
| Nitrophenol isomers | SH-β-CD | CdTe | Dynamic quenching caused by different inclusion complexes | [53] |
| **Chiral molecular sensing** | | | | |
| Tyrosine enantiomers | SH-β-CD | CdSe | Different fluorescent response based on hydrogen bonding induces different stabilization energy | [55] |
| Tryptophan enantiomers | SH-β-CD | Mn doped ZnS | Chiral fluorescence recognition due to different affinities of enantiomers to CD cavity | [56] |
| PNPG | β-CD | CdTe | Fluorescence quenching: *p*-nitrophenol from hydrolysis reaction of PNPG catalyzed by α-glucosidase could enter the CD cavity | [57] |
| Phenylalanine and tyrosine enantiomers | β-CD | CdSe/ZnS | Different association affected the process that combined the decrease in the FRET emission of dye and an enhancement in the CdSe/ZnS QDs luminescence | [58] |
| phenylalanine, tyrosine, tryptophan and histidine | β-CD | CdTe | Fluorescent decrease or increase due to the different binding energies of CD-amino acid enantiomer complexes | [59] |

**Abbreviations:** CD-Py: CD bearing pyrene on its secondary rim; MSA: mercaptosuccinic acid; S-β-CD: 11-[(ethoxycarbonyl)thio]undecanoyl-β-CD; Ts-β-CD: mono-6-(***p***-tolylsulfonyl)-CD; SH-β-CD: mono-6$^{b}$-thiol-β-CD; ***o,p***′-DDT: 1,1,1-trichloro-2-(o-chlorophenyl)-2-(***p***-chlorophenyl) ethane; ***p,p***′-DDT: 1,1,1-trichloro-2,2-bis-(***p***-chlorophenyl)ethane; PM-β-CD: permethylated β-CD; PNPG: ***p***-nitrophenyl-α-D-glucopyranoside.

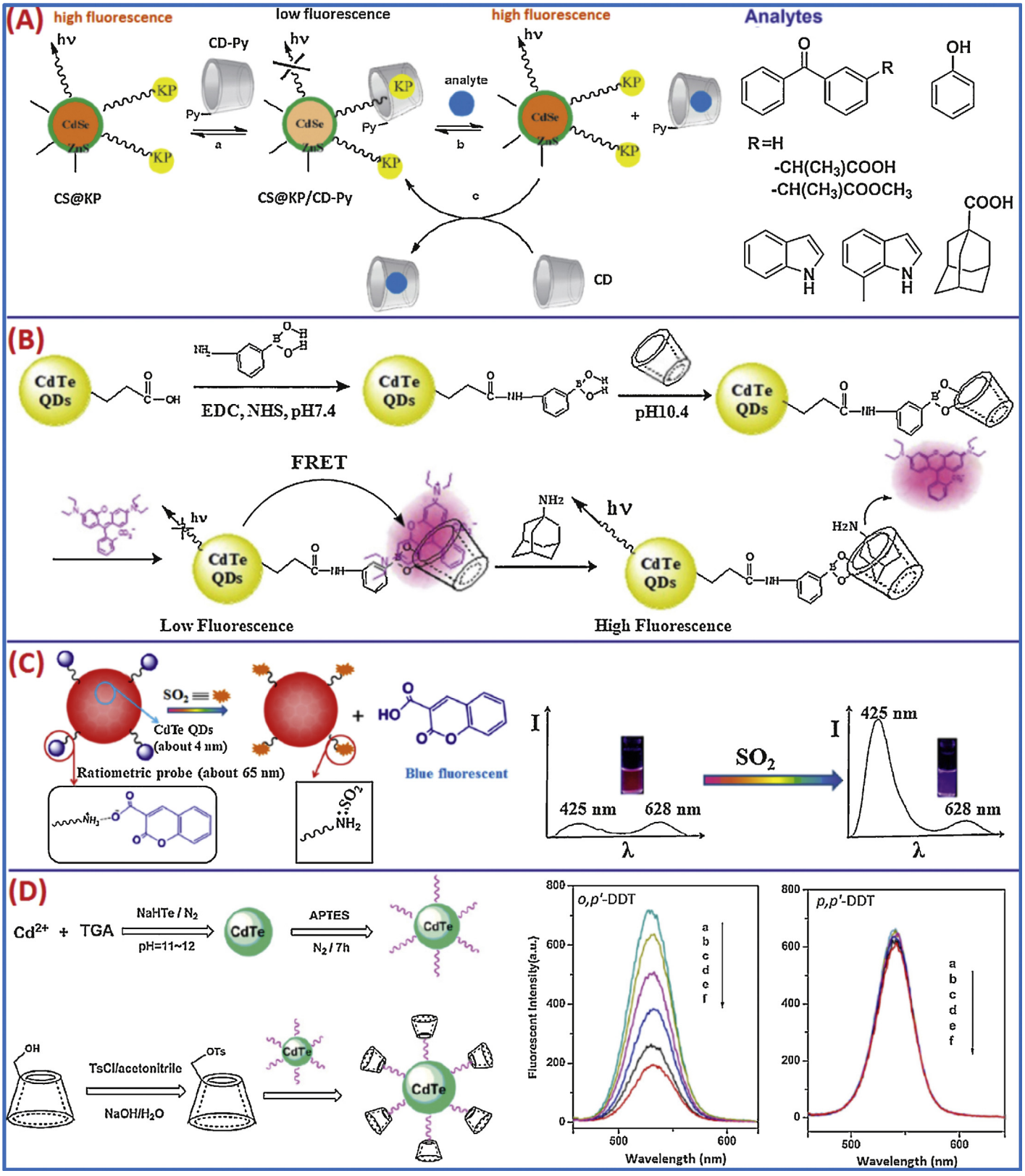


**FIGURE 2**

(A) Non-covalent CD based QDs probes for molecular determination by fluorescence recovery (Reprinted with permission from Ref. [47]. Copyright 2012 Royal Society of Chemistry). (B) QDs probes covalently linked CD for amantadine detection by shutting off the FRET path between QDs and Rhodamine B (Reprinted with permission from Ref. [48]. Copyright 2012 Elsevier); (C) The scheme to prepare aqueous fluorescent probes and the fluorescence emission response to different concentration of isomers (Reprinted with permission from Ref. [52]. Copyright 2012 Elsevier).

fluorescent probe achieved successful optical discrimination of *o,p′*-DDT and *p,p′*-DDT, which was attributed to their different association capacities resulting in distinguishable PL intensity decrease in response to increased isomer concentration (Fig. 2C). Our group developed CdTe QDs probes by directly binding SH-β-CD with unoccupied atoms on the surface [53]. Three nitrophenol isomers were optically recognized via a dynamic fluorescence quenching process.

### *The sensing of chiral molecules*

QDs capped with chiral molecule can endow the luminescent probes with chiral optical activity [54]. By virtue of their natural chirality, the fluorescent probes are able to chiral sense enantiomers, mainly focused on amino acids of biological interests. The optical detection of tyrosine enantiomers was explored using SH-β-CD directly binding CdSe QDs, wherein the L-enantiomer achieved better linearity than D-enantiomer over the concentration range from $1 \times 10^{-5}$ M to $4 \times 10^{-4}$ M [55]. In the analogy case of Mn-doped ZnS QDs capped with SH-β-CD, the photo-excitation at 315 nm can produce dual PL at 430 nm and 598 nm. This novel probes distinctively sensed tryptophan enantiomers: L-tryptophan displayed a large time-dependent enhancement in PL intensity, while D-enantiomer showed little effect [56]. In addition, β-CD-coated CdTe QDs were established for α-glucosidase activity assay and inhibitor screening. The hydrolysis product of the α-glucosidase reaction, p-nitrophenol, could quench the fluorescence emission via an ET process, whereas the fluorescence was turned on by α-glucosidase inhibitors [57]. By competitive association in CDs cavity with organic dye, the decrease in the FRET emission and an enhancement in CdSe/ZnS QDs luminescence can be simultaneously observed for phenylalanine and tyrosine enantiomers [58].

Our group reported a layer-by-layer strategy for silica-confined CdTe QDs with surface clicking with CD for chiral recognition (Fig. 3A–D) [59]. The as-prepared hybrid fluorescent sensor possessed stable and high fluorescent emission in pH rang of 6–14 due to the protection of silica shell (Fig. 3F). The chiral discrimination was implemented for four racemic pairs of amino acids (phenylalanine, tyrosine, tryptophan and histidine) at micromolar concentrations by taking advantage of the different binding energies of CD-amino acid enantiomer complexes, as revealed by density-functional theory calculation (Fig. 3G and H).

Although substantial efforts have been devoted into the CDs–QDs fluorescent probes, the use of functional CDs that have provided stronger molecular recognition in chromatography techniques is rare. On the other hand, the immobilization of CDs onto QDs surface is still to be developed using chemoselective reactions. The optical analysis of complex sample in real applications also requires from the efforts in building speedy, selective and sensitive fluorescent probes based on functional interfaces of nanomaterials.

## Ligands-driven ions sensing

Generally, the design principle of optical sensors for ionic species either in solution or in solid medium is mainly based on the replacement or direct interaction of surface ligands as described in these reviews [60–62]. We will emphasize and update the ingeniously designed interplay between surface ligands with ionic species for quantitative and qualitative detection.

### *Ions sensing in aqueous solutions*

By taking advantage of the dative chemistry, diversiform probes mostly for copper ($Cu^{2+}$), lead ($Pb^{2+}$), mercury ($Hg^{2+}$) ions have been fabricated based on the emulatory chelation occurred between QD surface and metal ions with ligands. By the recovery of quenched fluorescence of pristine CdSe/CdS QDs via shutting off the FRET pathway to surface anchored dithizone, trace $Pb^{2+}$ as low as $6 \times 10^{-12}$ M can be optically detected due to its stronger binding ability with dithizone (Fig. 4A) [63]. Conversely, the exfoliation of MPA from Mn-doped ZnSe/ZnS QDs leads to QDs aggregation (PL quenching) since MPA can act as a unique chelation acceptor for $Hg^{2+}$ [64]. The surface ligands can also determine the recognition mechanism of metal ions by controlling the interactions on interfaces, e.g. in the sensing cases of $Cu^{2+}$ using ZnSe QDs, a dynamic PL quenching process was found for glutathione [65], while a static PL quenching mechanism was concluded for mercaptoacetic acid (TGA) [66].

DNAs (oligonucleotides) are alternative ligands attributed to the formation stable complexes with metal ions by bridging specific nucleotide bases [67]. Zeng's group has demonstrated fluorescence "turn-on" [68] or "turn-off" [69] probes for $Hg^{2+}$ determination via $Hg^{2+}$-induced conformational change of a thymine-rich single-stranded DNA with Mn-doped CdS/ZnS QDs as fluorophores. The contrary recognition process is attributed to the different oligonucleotides with distinguishing interaction with $Hg^{2+}$ ions as depicted in Fig. 4B and C.

The design of QDs-based probes for inorganic ions can also be mediated by the adsorption of ions onto surface via the electrostatic attractions with ligands [70] or the replacement of ligands induced [71]. Besides, the reaction of metal ions with QDs core is also an effective approach to achieve fluorescent sensing. In the case of hexadecyl trimethylammonium bromide (CTAB) coated CdSe/ZnS QDs, the optical detection of $Cu^{2+}$ underwent a partial reduction to $Cu^{+}/Cu^{0}$ and the formation of $Cu_{x(x\,=\,1,2)}Se$ on QDs surface at the presence of thiosulfate, leading to the quenching of QDs emission [72].

In addition to ligands-determined sensing of $Cu^{2+}$, $Pb^{2+}$ and $Hg^{2+}$ ions, the recognition of some other inorganic species have also been reported. Butwong et al. utilized TGA capped CdS QDs to reduce $As^{5+}$ to $As^{3+}$, accompanied by quenched PL intensity. With the aid of sequential injection-stopped flow injection system, the total arsenic after reduction can be accurately determined [73]. Through the interaction with hydroxyl group with $Ba^{2+}$, 2-mercaptoethanol (ME) stabilized CdSe QDs presented increased fluorescence intensity due to the formation barium oxide on surface [74]. Impressively, ME can also be used as surface ligands to fabricate fluorescent probes for sensing anions such as cyanide ($CN^{-}$) and sulfide ($S^{2-}$) ions with little interference [75,76].

The monitoring of dual-emission fluorescence for hybrid QDs bearing another fluorophore can afford on-site visual determination of analytes. For example, the mesoporous silica-based sensing platform was prepared by comprising MPA coated CdTe QDs and poly(*p*-phenylenevinylene) [77]. The dual-emission at 500 nm and 717 nm gradually changed for the sensing $Cu^{2+}$ in the concentration range of 0–$1.6 \times 10^{-7}$ M. Besides, a novel ratiometric chemosensory probe was developed by embedding green-emitting CdTe QDs (550 nm) inside silica with further surface covalently linked with red-emitting MPA-CdTe QDs (650 nm) (Fig. 5A) [78]. The addition of $Cu^{2+}$ induced distinguishable color change due to the

changed intensity ratio of the two emission wavelengths even a slight decrease in 550 nm emission intensity. Unlike the ratiometric probe, the color change of single green MPA-QDs response to $Cu^{2+}$ was hard to observe (Fig. 5B). Impressively, the high selectivity for visual identification of $Cu^{2+}$ over other metal ions is achieved (Fig. 5C). For the practical detection of $Cu^{2+}$ residues existed on diarrhea leaves, a notable fluorescence color change from yellow-green to red was quickly observed under UV light (Fig. 5D). Such ratiometric fluorescence probe could be used to determine residues in herb products.

### *Ions sensing in solid state*

Although QDs-based chemosensory detections for metal ions are mostly accomplished in solutions, the solid sensing still has attracted particular attention for preparing visual and handy sensors. The adoption of 2-hydroxyethyldithiocarbamate (HDTC) to surface modify CdSe/ZnS QDs (HDTC-QDs) allowed the instant and on-site visual detection of trace metal ions either in solution or cellulose-acetate paper [79]. The surface chelating reaction between HDTC and $Hg^{2+}$ gradually turned the orange color of HDTC-QDs to red upon increased $Hg^{2+}$ concentration besides the reduced PL intensity (Fig. 6A). This fascinating work may help to fabricate portable unit for ions detection similar to pH paper. A commercially available biopolymer, chitosan, was used to stabilize ZnS QDs, which can be impregnated in chitosan film. The hybrid fluorescent film was applied in the detection or the removal of $Pb^{2+}$, $Hg^{2+}$ and $Ag^{+}$ in contaminated water based on the cation exchange. Characteristic bright yellow color pattern was

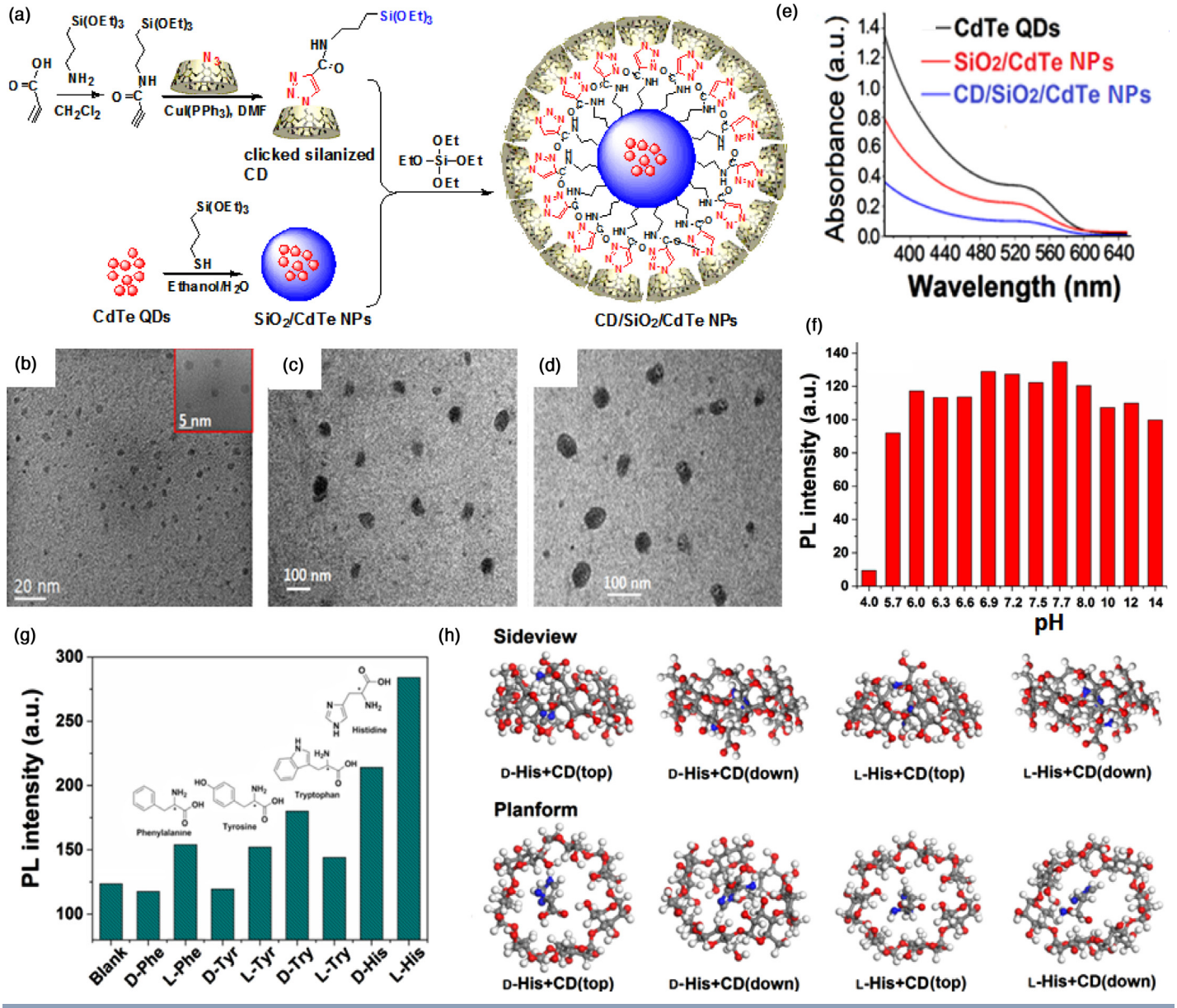


**FIGURE 3**

(A) Schematic presentation of the preparation of hybrid fluorescent probes; (B-D) TEM images of CdTe QDs, $SiO_2$/CdTe NPs and CD/QDs $SiO_2$/CdTe NPs; (E) The absorbance spectra of CdTe QDs, $SiO_2$/CdTe NPs and CD/QDs $SiO_2$/CdTe NPs; (F) The PL intensity of fluorescent probe with varying pH from 4.0 to 14; (G) The PL intensity of fluorescent probe response to the addition of different enantiomers; (H) Optimized structure of the complex between CD and tryptophan and histidine enantiomers from sideview and platform (Reprinted with permission from Ref. [59]. Copyright 2016 Royal Society of Chemistry).

exceptionally observed for $Hg^{2+}$ ion corresponding to the formation of HgS, while brown color was gained for $Pb^{2+}$ and $Ag^{+}$ (Fig. 6B). Unfortunately, the applicability of QDs-based solid sensors to real samples is still limited by the lack of selectivity since some metal ions possess similar effect on luminescence of QDs [80].

The assembly of QDs on an electrode is another efficient strategy to fabricate photoelectrochemical (PEC) sensors. The use of probe DNA (oligonucleotides) can integrate CdS QDs on the surface of Au NPs labeled target DNA. The photocurrent was changed upon the addition of $Hg^{2+}$ undergoing an ET principle process mediated by the T–$Hg^{2+}$–T pairs [81]. It is noteworthy that the solid-state chemiluminescent assay combining liquid-phase microextraction and microfluorospectrometry proposed by Bendicho' group [82] is helpful to improve the selectivity and sensitivity of the chemiluminescence (CL) response to $Sb^{3+}$ and $As^{3+}$ for CdSe QDs (Fig. 6C). The ligands acted as energy donor with QDs acceptor in an energy transfer process. Hexadecylamine, proved to be the most suitable option for the energy transfer compared to TOPO, dodecyl sulfide, L-cysteine and TGA. Amongst of ions tested, inhibition of CL was

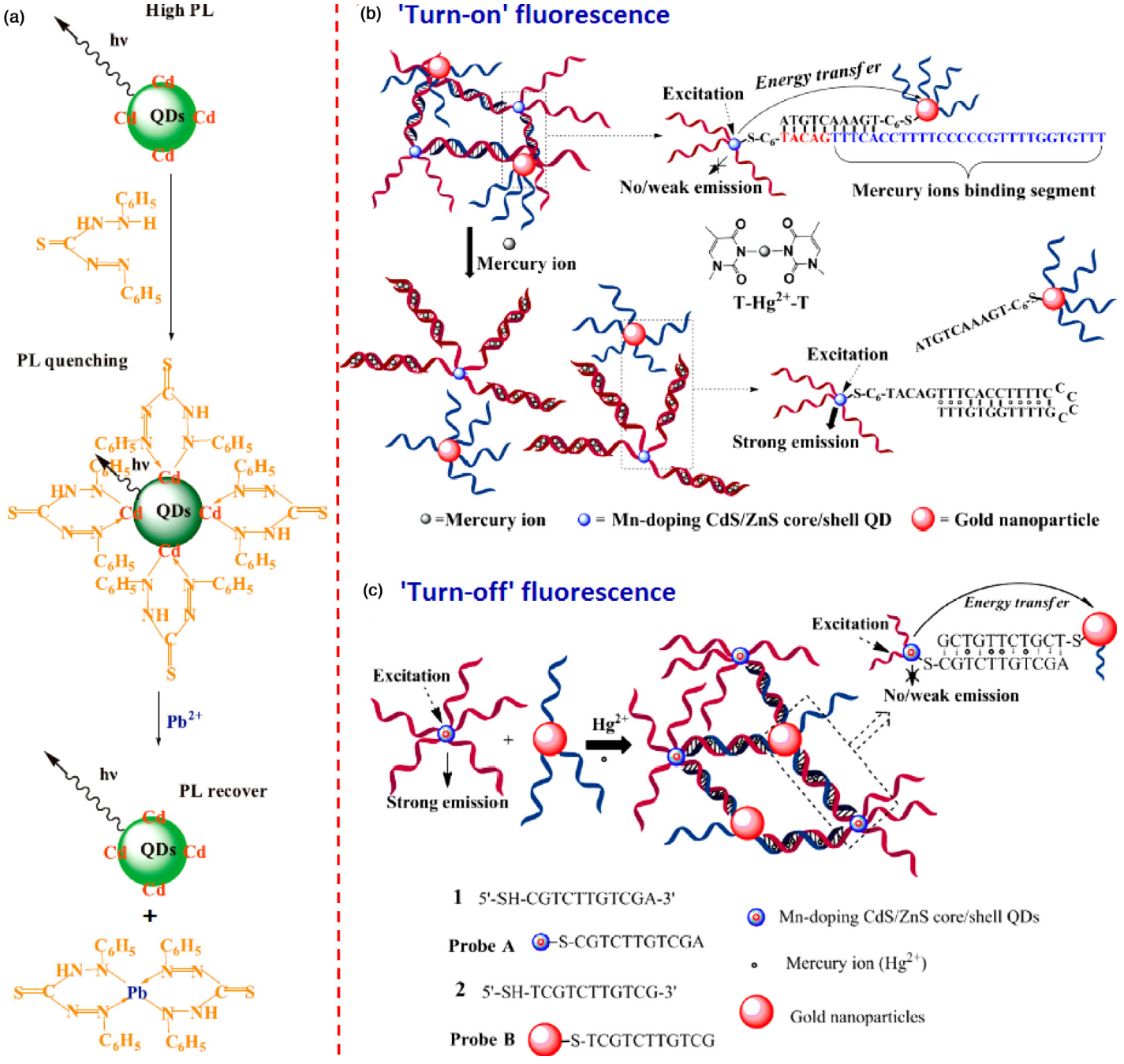


**FIGURE 4**

(A) Switched fluorescence mechanism for the detection of $Pb^{2+}$ via emulatory chelation (Reprinted with permission from Ref. [63]. Copyright 2013 Elsevier); (B) Schematic description of the "turn-on" and "turn-on" fluorescence based on the $Hg^{2+}$-mediated formation in DNA duplexes (Reprinted with permission from Ref. [68]. Copyright 2013 American Chemical Society and Ref. [69]. Copyright 2013 American Chemical Society).

observed for Sb, Se and Cu ions. As revealed in AFM images, the increased size encountered for samples without $Sb^{3+}$ corresponded to the formation of a $SeO_2$ layer over CdSe QDs surface, which did not occur in the samples containing $Sb^{3+}$.

## Surface engineering for biological applications

On the interface between QDs and biological environment, the ligands are of vital significance for controlling water-dispersibility, biocompatibility and bioconjugation. At current stage, the widely adopted strategies in engaging QDs surface for biological purpose comprise the coating of silica shell, encapsulation of amphiphilic ligands and ligands exchange.

### *Surface coating with silica shell*

The ligand exchange for the transfer of hydrophobic QDs into aqueous medium is, sometimes, accompanied with a drastic decrease in the luminescence yields. To compensate the loss of PLQY, the direct encapsulation of QDs with silica shell is an effective approach. The silica layer capped on QDs surface usually endows them with outstanding aqueous stability and controlled size and fluorescence by silica thickness [83]. The silica shell can act as platform for the further coating of other nanoparticles. For instance, the coating with a continuous gold nanoshell can provide QDs with stable and Poissonian emission at room temperature regardless of drastic changes in the environment (Fig. 7A) [84]. Besides, versatile functionalities can be imported on the outer surface of silica. Goftman et al. decorated the surface of CdSe/CdS/ZnS QD@$SiO_2$ with or carboxy and epoxy groups and polyethylene (PEG) [85]. The conjugation of functionalized QD@$SiO_2$ with IgG by means of EDC/NHS activation enables the fluorescent probe in the immunoassay detection of mycotoxin DON (Fig. 7B). The great potential in bioimaging such as in vivo and in cell tracking have emerged for QDs embedded in silica [86,87]. Silica-coated, QD-embedded silica NPs (Si@QDs@Si NPs) containing CdSe@ZnS or CdSe@CdS@ZnS QDs were ingeniously prepared, demonstrating unique structure-based advantages in vitro or in vivo imaging over single QDs that have a similar quantum yield [88] (Fig. 7C). Si@QDs@Si NPs were suitable for the in vivo imaging due to the highly amplified fluorescence signals and less toxic than equivalent numbers of silica-free single QDs. Moreover, the Si@mQDs@Si NPs containing multilayered QDs can allow the detection of as few as 400 labeled cells in mouse skin. Thus, the encapsulation of QDs in silica shell is proven to be useful in biomedical fields, particularly for the bioimaging of in vivo cell tracking, which requires a high sensitivity.

### *Encapsulation of amphiphilic ligands*

Upon the aware of their multi-interactions with QDs, the polymer ligands have been intensively exploited to produce more stable fluorescent probes under complex and biological conditions covering a broad range of pH and ionic strengths. The amphiphilic molecules possess hydrophobic groups for interacting with pristine ligand and hydrophilic groups providing water solubility. These polymers also provided flexibility of functionalization (tuned type and number of functional groups) and additional barrier to control permeability of the QDs. One popular category of amphiphilic ligands for encapsulating QDs is maleic anhydride-based alternate polymers. The capacity to conjugate molecular units of maleic anhydride renders QDs with anticipant functionalities, like photochromic compounds tuned FRET [89] and pyridine motifs enhanced optical performance [90]. The applicability of such amphiphilic polymer in immunoassay was verified using QDs encapsulated by three polymers include PSMA-Jeffamine M1000, PMAO-Jeffamine M1000 and PMAO- Jeffamine ED-2003

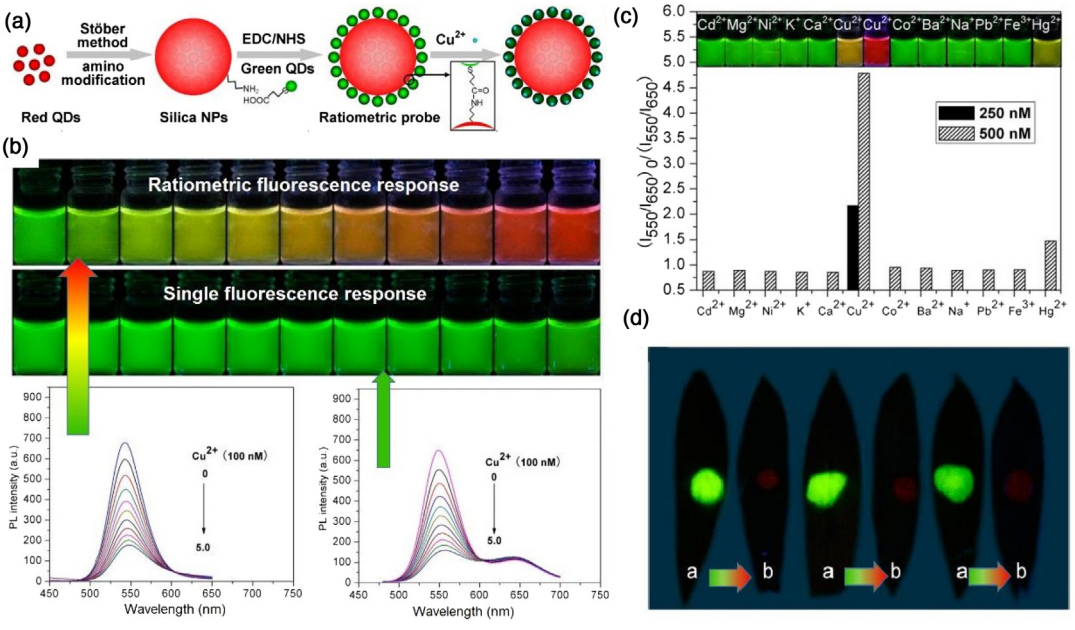


**FIGURE 5**

(A) Schematic depiction of the ratiometric probe; (B) The fluorescence colors and the corresponding fluorescence spectra ($\lambda_{ex}$ = 365 nm) of ratiometric probe and single green MPA-QDs response to different concentrations of $Cu^{2+}$; (C) The selectivity of ratiometric probe to various metal ions in the HEPES buffer (pH = 7.4, 10 mM) at 250 nM (black bar) and 500 nM $Cu^{2+}$ (striped bar); (D) The fluorescence images of the ratiometric probe on the surface of untreated (green) and treated (red) diarrhea leaves (Reprinted with permission from Ref. [78]. Copyright 2013 American Chemical Society).

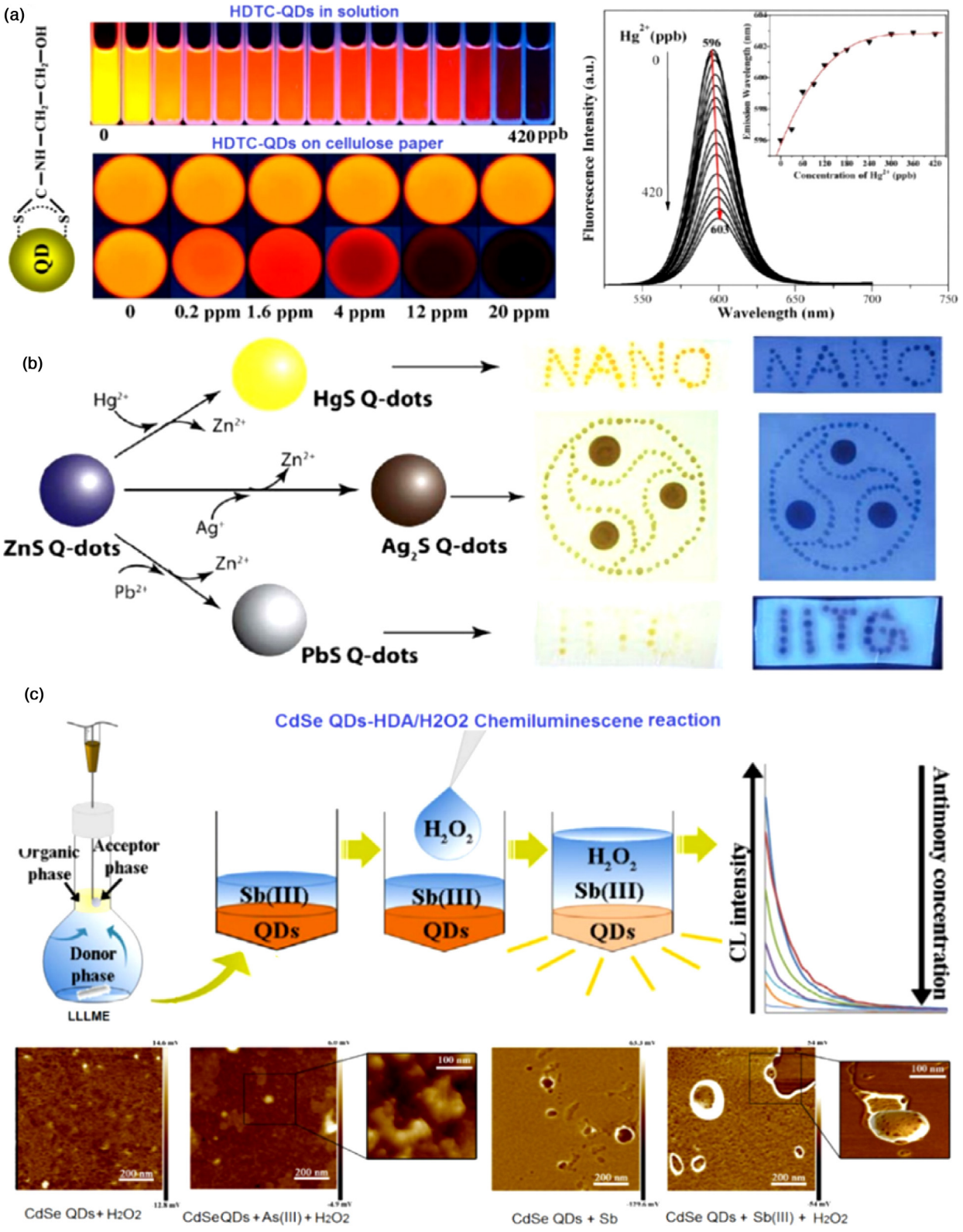


**FIGURE 6**

(A) Fluorescence images of HDTC-QDs in solution and on cellulose paper upon the addition of different amounts of aqueous $Hg^{2+}$ ions with the corresponding fluorescence spectra in solution, the inset revealed the emission shifts response to the $Hg^{2+}$ concentration (Reprinted with permission from Ref. [79]. Copyright 2012 American Chemical Society); (B) The cation exchange of different metal ions with ZnS-QDs and the photos of as-fabricated film under visible and UV light (Reprinted with permission from Ref. [80]. Copyright 2012 American Chemical Society); (C) Schematic representation of the LLLME-CL system for Sb determination with AFM images for CdSe QDs + $H_2O_2$, CdSe QDs + As(III) + $H_2O_2$, CdSe QDs + Sb and CdSe QDs + Sb(III) + $H_2O_2$ (Reprinted with permission from Ref. [82]. Copyright 2013 Elsevier).

as depicted in Fig. 8A [91]. Another appealing series of amphiphilic ligands is the block polymers derived from poly(isoprene)-*b*-poly(ethylene glycol) (PI-*b*-PEG) and poly(isoprene-block-ethylene oxide) (PI-b-PEO) pioneered by Weller's groups [41,92–94]. Different from the direct encapsulation of second ligand layers based on hydrophobic effects, the three-step coating using block polymers consists of a partial ligand exchange of native ligands by poly(isoprene)-diethylentriamine (PI-$N_3$), a subsequent addition of poly(isoprene)-b-poly(ethyleneglycol) diblock copolymer (PI-b-PEG) to transfer QDs to water and final cross-linking undergoing a radical initiated reaction (see Fig. 8B) [93].

By taking advantage of the nontoxicity and water solubility of PEO, PI-b-PEO and PI-b-$(PEO)_2$ were developed to reduce unspecific protein absorption provides a good biocompatibility [95]. The

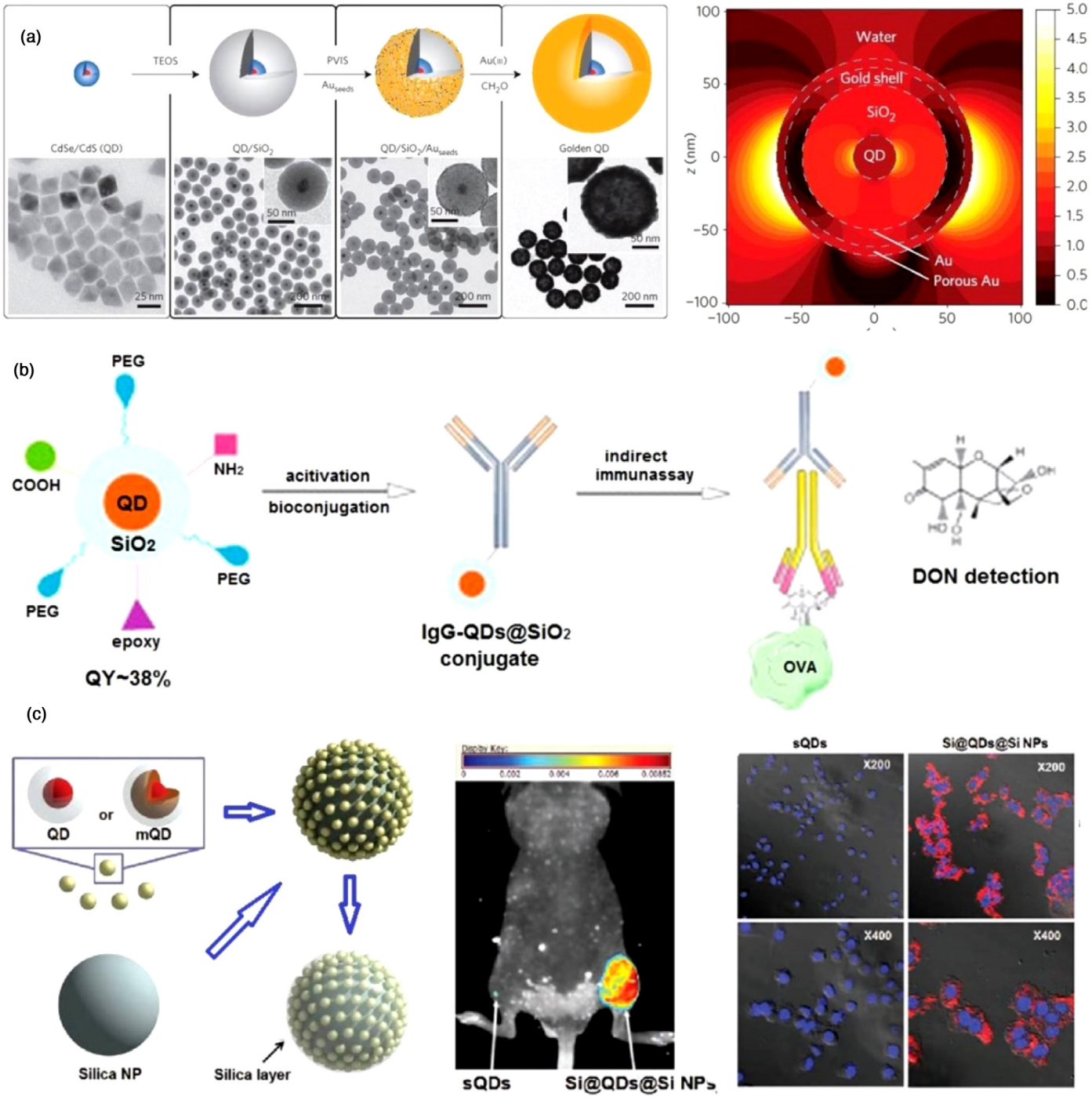


**FIGURE 7**

(A) Schematic representations of the growth on QD surface and corresponding TEM images and the field distribution dominated by the dipolar mode for final golden QDs (Reprinted with permission from Ref. [84]. Copyright 2015 Nature Publishing Group); (B) Schematic depiction of functionalization on QDs/$SiO_2$ for immunoassay of mycotoxin DON (Reprinted with permission from Ref. [85]. Copyright 2016 Elsevier); (C) Schematic route of the preparation of Si@QDs@Si NPs (left), fluorescence image a BALB/c nude mouse with 2 pmol QDs were injected (middle) and cellular uptake in vivo test (right) (Reprinted with permission from Ref. [88]. Copyright 2013 Wiley).

polymer size mediated unspecific uptake of A549 cells was observed except for the biggest ligands as shown in Fig. 8C. Meanwhile, highest reactivity of $Cu^{2+}$was observed PI-b-$(PEO)_2$ proven by TEM element mappings (Fig. 8D). With the conjugation of carbohydrates on the end tail of polymers, the QDs can be afforded great potential in signaling cascades, cellular recognition and molecular and cellular targeting [41] (Fig. 8E).

Practical applications demonstrated the above-mentioned polymers ligands may be more suited for single particle imaging applications. Facing more complex applications such as QD cellular delivery, QDs prefer to be packaged in dozens rather than single individual fashion. Recently, Park et al. [40] developed amphiphilic polyethyleneimines (PEIs) to encapsulate dozens of QDs with a positive outer surface and a hydrophobic inside pocket, rendering the whole entity with a hydrodynamic diameter of ~100 nm. As shown in Fig. 9, the positive outer surface of QD-amPEI can be used for the co-delivery of QDs and GFP silencing RNAs by assembling siRNAs to the outer surfaces and cell-specific targeted labeling which showed the specific-to-nonspecific signal ratio over 100. The inside hydrophobic compartment was further applied for cohosting oxygen sensing phosphorescence Ru dyes along with QDs.

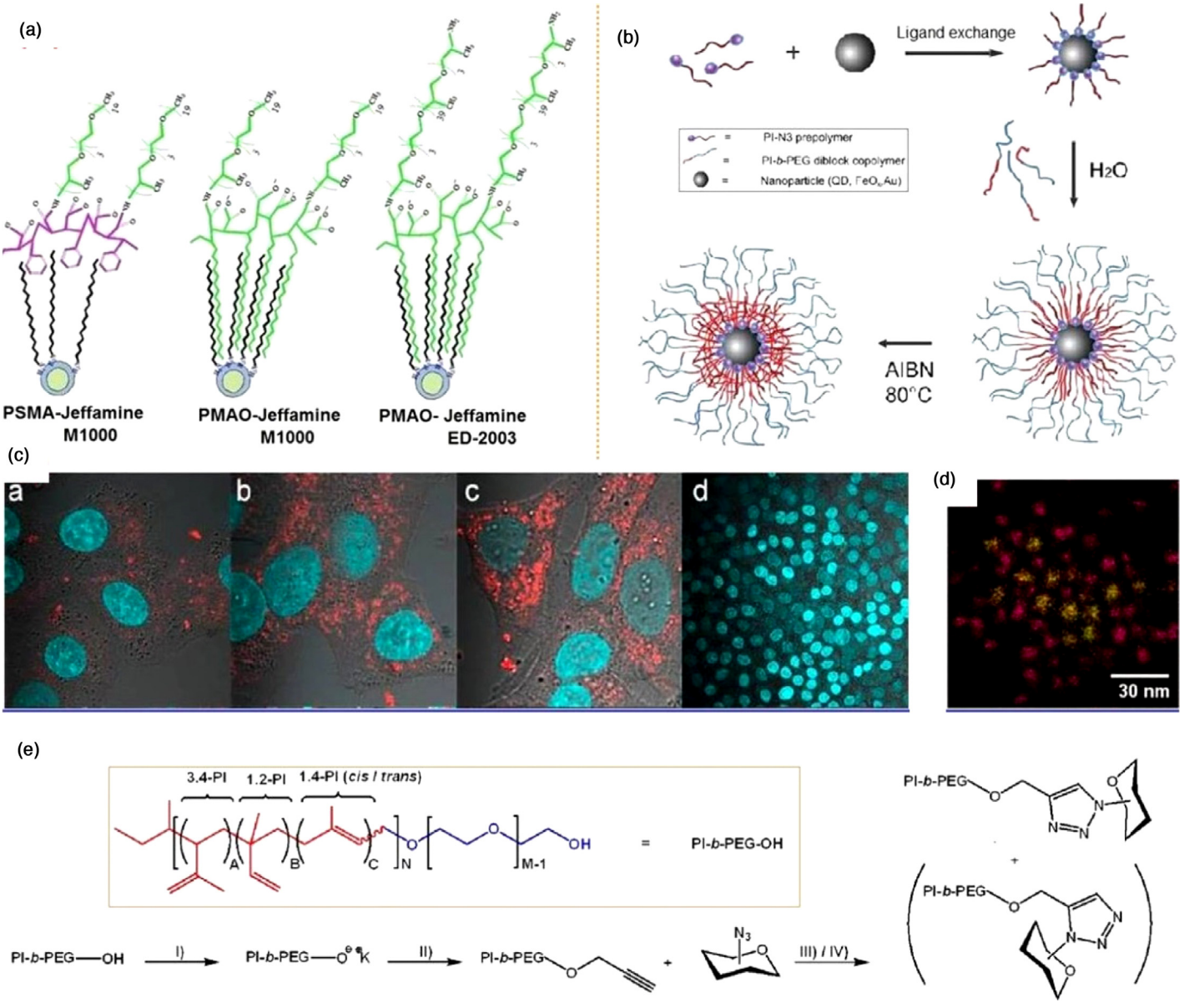


**FIGURE 8**

(A) Schematic illustration of the direct encapsulation of hydrophobic QDs using three maleic anhydride-based alternate polymers for immunoassay (Reprinted with permission from Ref. [91]. Copyright 2014 Elsevier); (B) Schematic depiction of three-step encapsulation of QDs undergoing a radical initiated reaction with block polymers (Reprinted with permission from Ref. [93]. Copyright 2013 American Chemical Society); (C) Confocal microscope images A549 cells incubated with 1 μM of PI-b-PEO encapsulated QDs after 20 h and (D) Scanning transmission electron microscopy (STEM) measurements of the copper incubated (2000 equiv. pp) encapsulated QD: overlay of the cadmium L (yellow) and copper K (magenta) signals of PI-b-$(PEO)_2$ encapsulated particles (Reprinted with permission from Ref. [95]. Copyright 2013 American Chemical Society); (E) Schematic route of the tail engineering for conjugation of carbohydrates via click chemistry (Reprinted with permission from Ref. [41]. Copyright 2013 American Chemical Society).

In addition to polymer ligands, the amphiphilic phospholipid vesicles or liposomes with hollow spherical structure and high loading capacity make them alternative for packaging QDs. Unfortunately, the adoption of liposomes in vivo applications and storage encounters dramatic instability and high sensitivity toward external medium. The disadvantage can be overcome by further coated with a layer of silica [96]. A single CdSe/CdZnS QD can be encapsulated into per phospholipid micelle and allowed further coupling functional molecules for in cellular and in vivo imaging according to Dubertret's protocol [97]. More recently, a dual solvent exchange method was proposed using a small amount of phospholipid-PEG to form water-dispersible QD solutions. The coating efficiency and quality were simultaneously improved with ascending polarity, resulting in large and irregular-shaped QDs [98]. The packing QDs of can also be performed within phospholipid membranes with altered membrane structure, whilst the physical state of membrane in turn controlled the optical and chemical properties of QDs [99]. Yong's group successfully utilized single PEGylated phospholipid micelle to encapsulate more than one infrared emitting ultra-small PbS QD as depicted in Fig. 9A [100]. The reduced cytotoxicity of these fluorescent materials was evaluated by MTS assay as well as histological analysis studies (Fig. 10B and C). Their applicability was also further demonstrated by the study of in vitro and in vivo bioimaging (Fig. 10D and E). It is noteworthy that an amphiphilic protein (hydrophobin) has proved as alternative option for stabilizing QDs in biological medium. The advantages of the biological ligands with available functional groups were highlighted for both in vivo cancer cells imaging and other imaging applications [101].

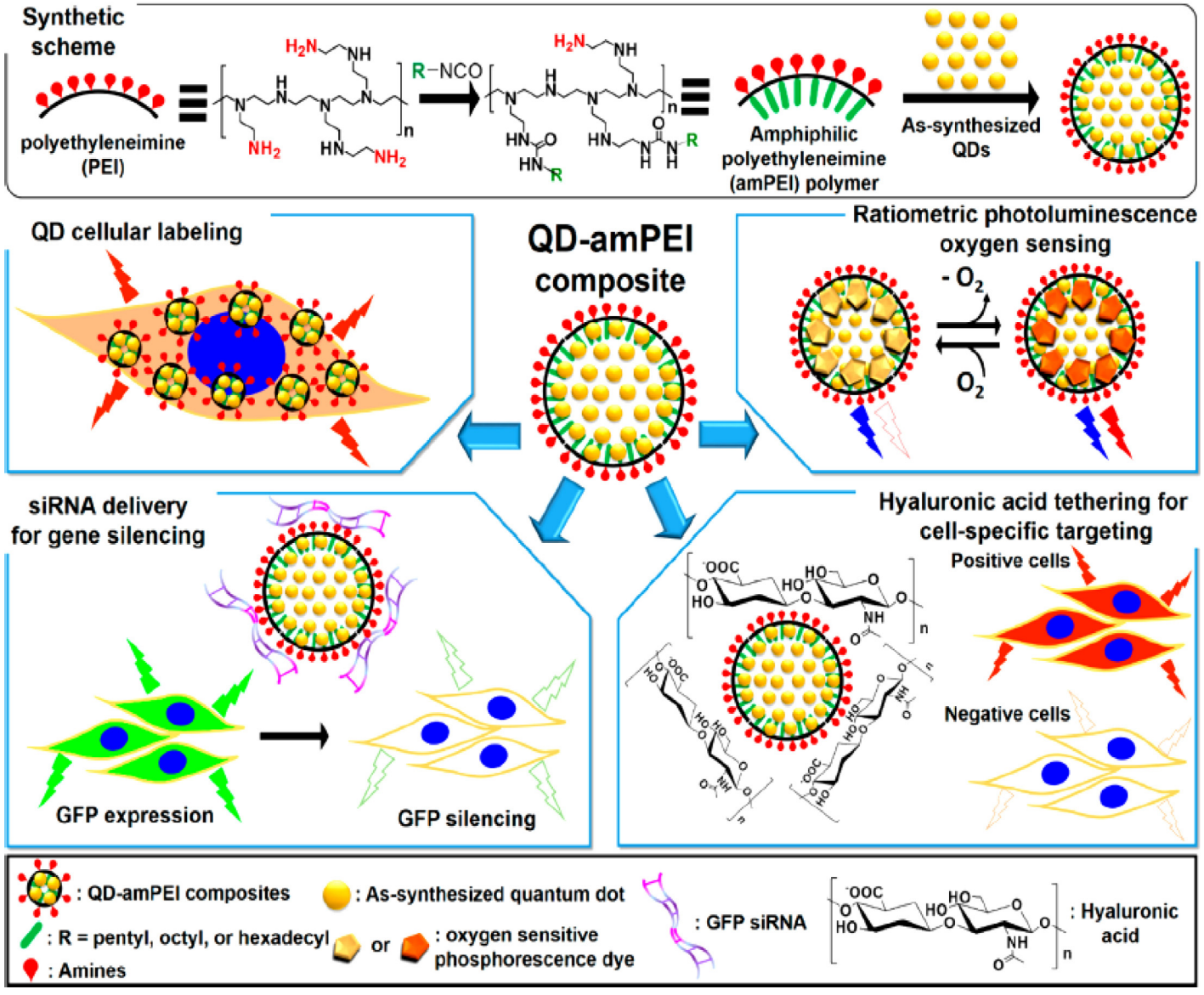


**FIGURE 9**

Schematic representations for the synthesis of amphiphilic polyethyleneimine derivatized polymer (amPEI) and the encapsulation of dozens of QDs in amPEI for QD_amPEI composite preparation (top), and demonstrated QD_amPEI platform applications: QD cellular labeling, siRNA delivery for GFP gene silencing, hyaluronic acid tethering for cell-specific targeting, and ratiometric photoluminescence oxygen sensing (from upper left box to counterclockwise order). (Reprinted with permission from Ref. [40]. Copyright 2015 American Chemical Society).

*Multidentate ligands for ligands exchange*

Monodentate ligands referring to small organic molecules allow only one interaction site to bind QD surface. The ligands possessing multi-coordinating groups (i.e. multidentate ligands) can enhance the colloidal stability of QDs by complementing the chelate effect on surface. As the representative bidentate ligands, dihydrolipoic acid (DHLA) derived from lipoic acid (LA) can lengthen the storage and stability of QDs, but this advantage is limited to basic medium since the solubility is greatly dependent on the deprotonation of the carboxyl group. This limitation can be overcome with the complement of PEG polymer, providing QDs with significant stability from pH 5 to 12 for over 1 year by virtue of the broad range pH solubility of the polymers segment [102].

In this aspect, a novel tridentate ligand appended with PEG was ingeniously synthesized and enabled near infrared-emitting QDs in vivo imaging [103]. More recently, DHLA-based ligands bearing zwitterion moieties have ever-increasingly been adopted for the ligands exchange, affording reduced hydrodynamic size for

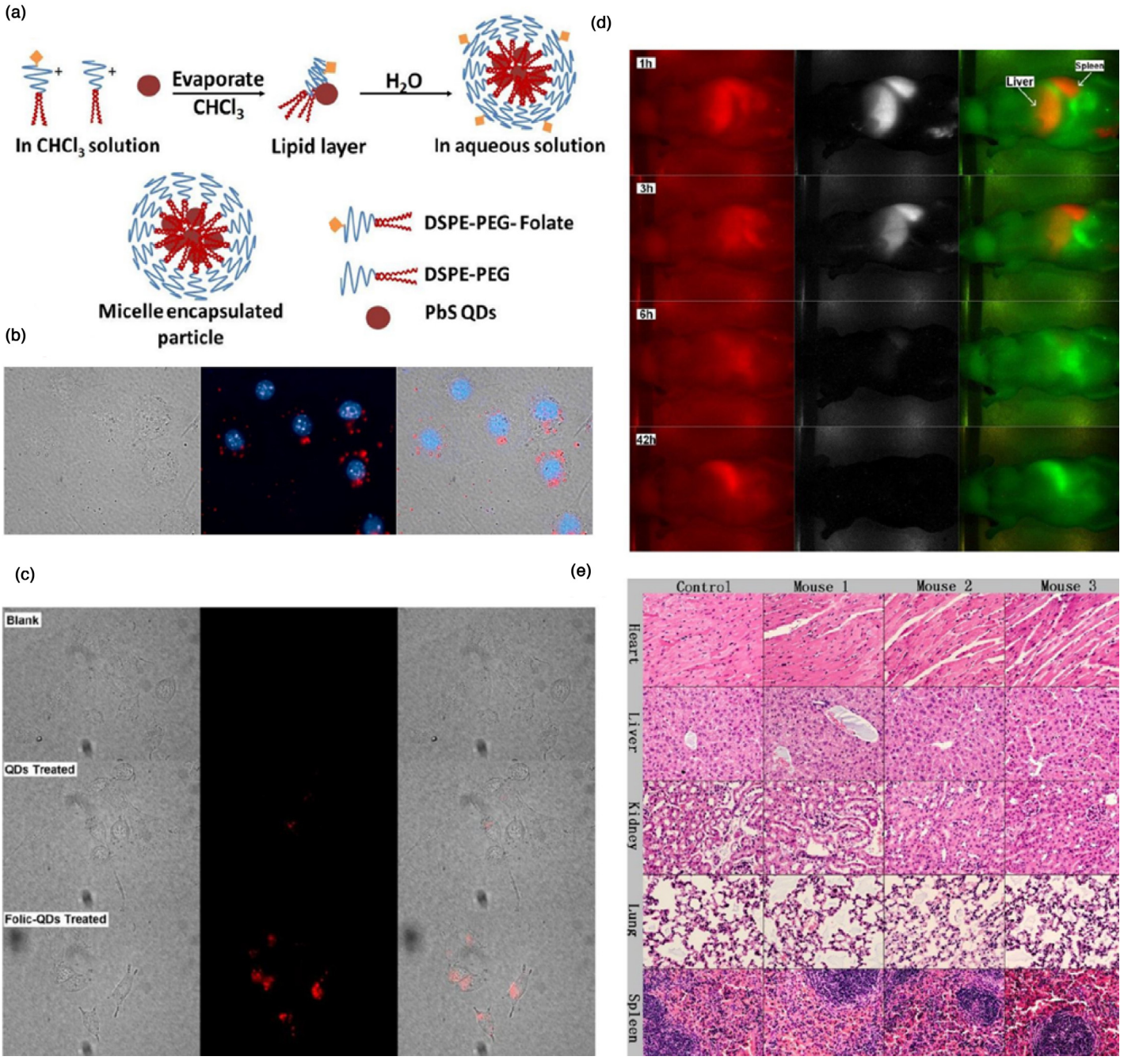


**FIGURE 10**

(A) Schematic illustration of the PEGylated phospholipid micelle encapsulation of PbS QDs; (B) RAW264.7 macrophages labeled with micelle-encapsulated PbS QDs (red), the cell nucleus is stained with Hoechst 33342 (blue); (C) Images of MiaPaCa-2 cells treated with folic acid functionalized micelle-encapsulated NIR PbS QDs; (D) In vivo fluorescent images of a nude mouse tail vein injected with PEGylated phospholipid micelle encapsulated PbS QDs with original unprocessed images (left), QDs signal channel (middle) and pseudo-colored images of the spectrally separated signals (right); (E) Histological studies on the major organs of the QDs injected mice at a dosage of 25 mg/kg after 4 weeks (Reprinted with permission from Ref. [100]. Copyright 2012 Ivyspring).

QDs [104–106]. Mattoussi's group proposed a general photoligation strategy for LA-based zwitterionic ligands-controlled phase transfer of QDs, providing high PLQY and excellent colloidal stability over acidic to basic pH, and excess salt concentration [107]. The small lateral extension of the capping layer allowed QDs to conjugate globular proteins in acidic as well as basic conditions. They also extended the concept of irradiation-induced phase transfer to the ligands that have two lipoic acid groups (Fig. 11) [28,108]. The thin ligand layer can allow the direct access of terminal polyhistidine in proteins the QD surface confirmed by amylose affinity chromatography through metal affinity-driven interactions. A FRET interactions quenched emission of QD was also observed with histidine-tagged mCherry fluorescent proteins.

Cumulatively, the polymers containing multiple coordinating sites such as thiols, imidazole or pyridine groups have been regarded as comparable ligands to multidentate small-molecular-substrates. The use of thiol-terminated ligands inevitably suffers from photo-oxidation during extended storage time leading to the ligand desorption from the QD surface, whilst the imidazole and pyridine exhibit stronger resistance against photo-oxidation despite of weaker coordination affinity. The multidentate polymer ligands containing diversified binding motifs can not only overcome the colloidal stability and photobleaching but also minimize the hydrodynamic size of QDs [110]. Poly(acrylic acid) bearing a ratio of pyridines to PEG has been reported for one- or two-steps ligands exchange [109] (Fig. 12A). The QDs with exposed carboxyl groups enabled the coupling of Lissamine rhodamine B ethylenediamine (RhB) to facilitate FRET from the QD donor to the dye acceptor. Meanwhile, the direct assembly of His-tagged proteins on the outer was also satisfied (Fig. 12B). Biocompatibility and long-term stability of the pyridine polymer coated QDs were evaluated by the cellular delivery via both microinjection and peptide facilitated uptake along with intracellular single QD tracking studies and cytotoxicity testing.

In this aspect, poly(isobutylene-alt-maleic anhydride) (PIMA) which has been adopted in amphiphilic ligands is also applicable

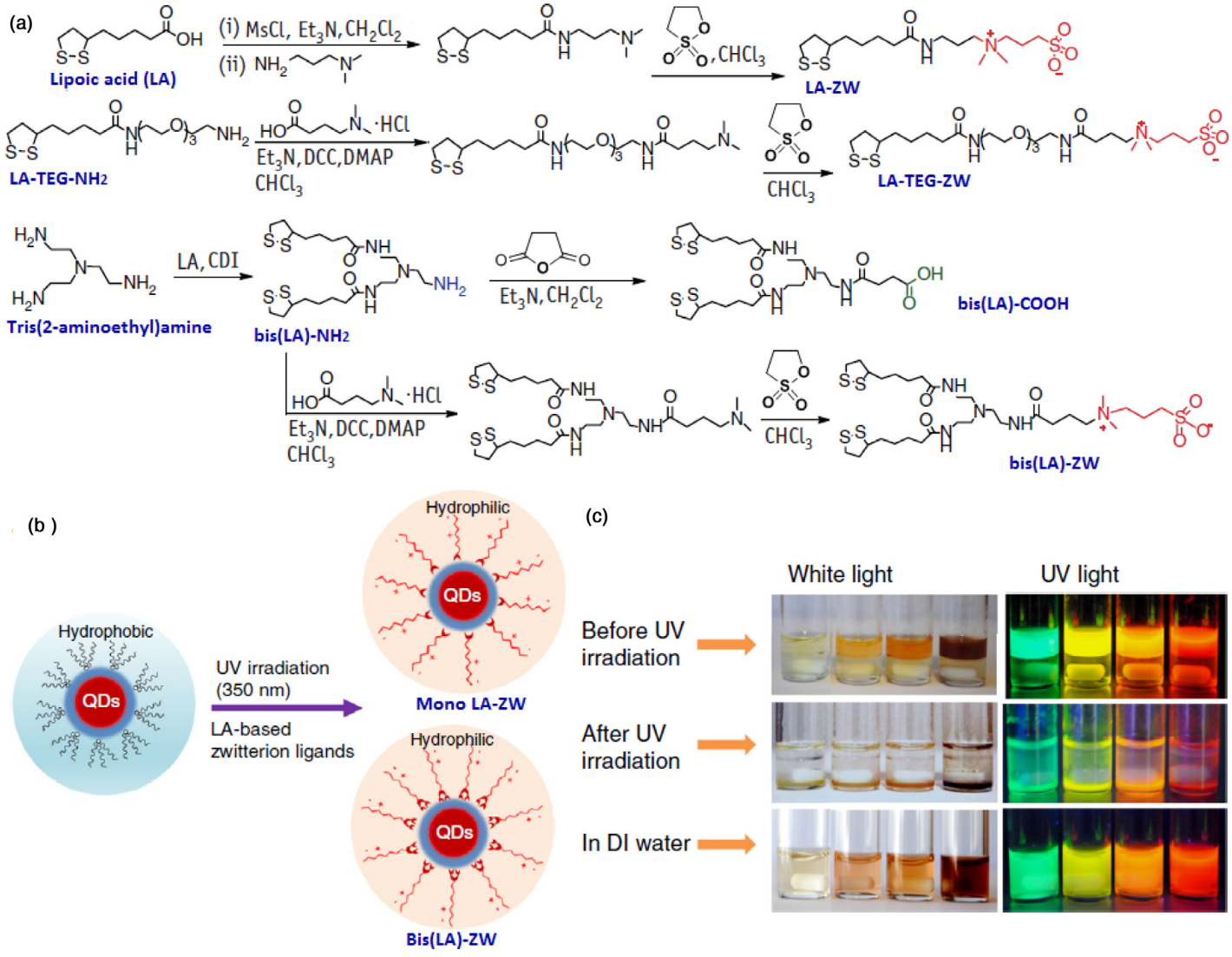


**FIGURE 11**

(A) Schematic description of the synthetic routes used to prepare the various zwitterion ligands; (B) Schematic representation of the photoligation strategy applied to the hydrophobic QDs (capped with TOP/TOPO, phosphonic acid and alkylamines) with LA-ZW and bis(LA)-ZW. (C) Images of a set of QDs of different sizes (with $\lambda_{em}$ = 540, 574, 585 and 624 nm) transferred from hexane (top layer) to methanol (bottom layer) and finally dispersed in water; the ligand exchange was carried out using LA-ZW. (Reprinted with permission from Ref. [28]. Copyright 2015 Nature Publishing Group).

for synthesis of multidentate polymer ligands. PIMA bearing lipoic acid and histamine is efficient for photoligation induced in situ ligand exchange under borohydride-free conditions [37,111]. These multidentate polymers can provide maintained PL intensity in water as that in hexane and long-term stability in a broad pH range (3–13) at nanomolar concentration under ambient conditions (Fig. 13A–C). Besides, the fluorescent QDs probes can be endowed with additional multiformity such as FRET process, pH-controlled luminescence, and intracellular uptake with no cytotoxicity by turning the terminated functionalities (Fig. 13D–G). The chemical engineering on the side chain of PIMA backbone offer great potential for bioconjugation. Besides the EDC/NHS mediated conjugations and His-Tag-based self-assembly above-mentioned [91,109,111], metal-free strain-promoted click chemistry of high selectivity is strongly recommended for coupling biomolecules [35,37,112]. The bio-orthogonal functionalities of (aldehyde and azide) can specifically couple two distinct targets with great specificity [37].

The advantage of multidentate polymer ligands over bidentate zwitterionic ligands is revealed by Giovanelli et al., higher affinity for long-term bioimaging was obtained for the former [113]. However, a comprehensive study of multidentate polymers and small-molecular ligands is required with a battery of assay related to biological applications.

## Summary and outlook

Above we review the progress in the development of semiconductor QDs-based chemosensors and biosensors in recent five years. We can strengthen the understanding about the role of surface ligands playing in not only controlling the colloidal stability but also tuning the fluorescence emission behaviors of QDs, the energy transfer between QDs and extraneous acceptor/donor can be thus easily mediated by altering the ligands types and assembly QDs surface. Also, the multiform functionalities on ligands endow QDs probes with superior selectivity and sensitivity. However, many enormous challenges still exist in developing QDs-derived fluorescent materials for practical applications, which may include the followings. (I) The lack of selectivity against varying interferences limits the practical detection ions and molecules in real samples from contaminated lakes, factory sewage or food residue. By altering the surface ligands to improve the selectivity, the rapid and handy QDs-probes for ions like pH paper might be realized [79]. (II) The sensing of small molecules, especially the amino acids in solution is impressive. But the target probing of biomolecules such as thiols, amino acids, peptides and proteins using QDs is still under exploration, compared to the chemosensors based on organic chromophores [114]. The engagement of QDs surface by introducing the reaction sites for thiols with high specificity is recommended. The tethering of supramolecules on QDs surface is

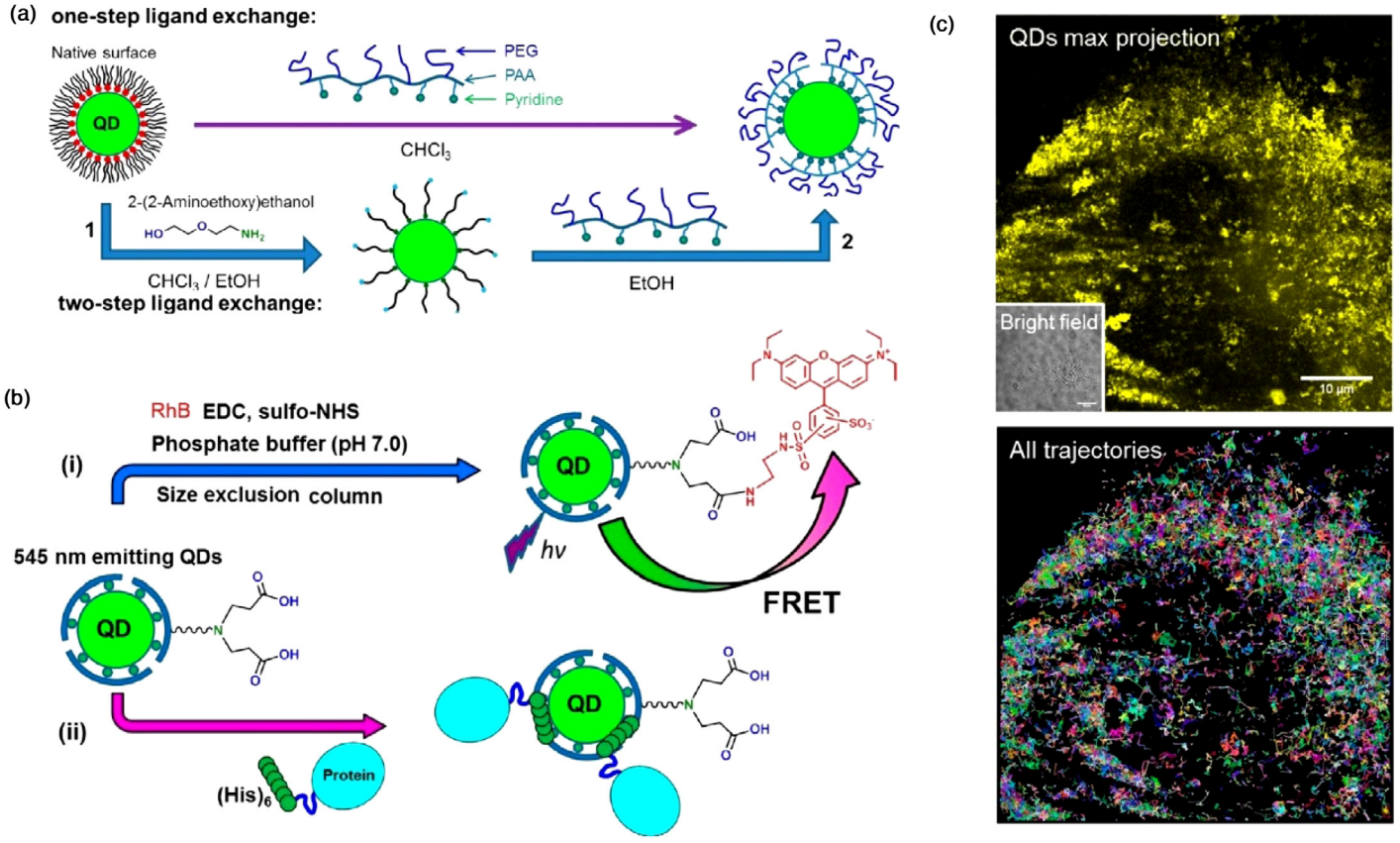


**FIGURE 12**

(A) Schematic depiction of the one-step and two-step ligand exchange processes; (B) The conjugation of Lissamine rhodamine B ethylenediamine (RhB) and direct assembly of His-tagged proteins; (C) Intracellular single QD tracking with max projection and trajectory mapping of select QD microinjected into the cytoplasm of U2OS cells imaged by HILO microscopy. (Reprinted with permission from Ref. [109]. Copyright 2014 American Chemical Society).

also of great possibility to achieve the recognition of proteins via the ''host–guest'' interactions with side chain. The construction of multiple molecular interactions (e.g. hydrogen bonding, dipole-dipole interactions, etc.) might be helpful for enhanced specific recognition, which has been proven by the improved chiral separations using selectively modified CDs [46]. (III) The toxicity is critical for the biological applications. Synthesis of new nontoxic and environmentally friendly QDs such as cadmium-free QDs is feasible [115]. On the other hand, the building of a roadmap for interrogating the wide-ranging toxicity data of existing QDs is helpful to guide the design of engineered QDs and to predict the toxicity [116]. Facing the challenge for in vivo bioimaging requiring high spatiotemporal resolution and penetration depths, the development of near-infrared (NIR) and short-wavelength infrared

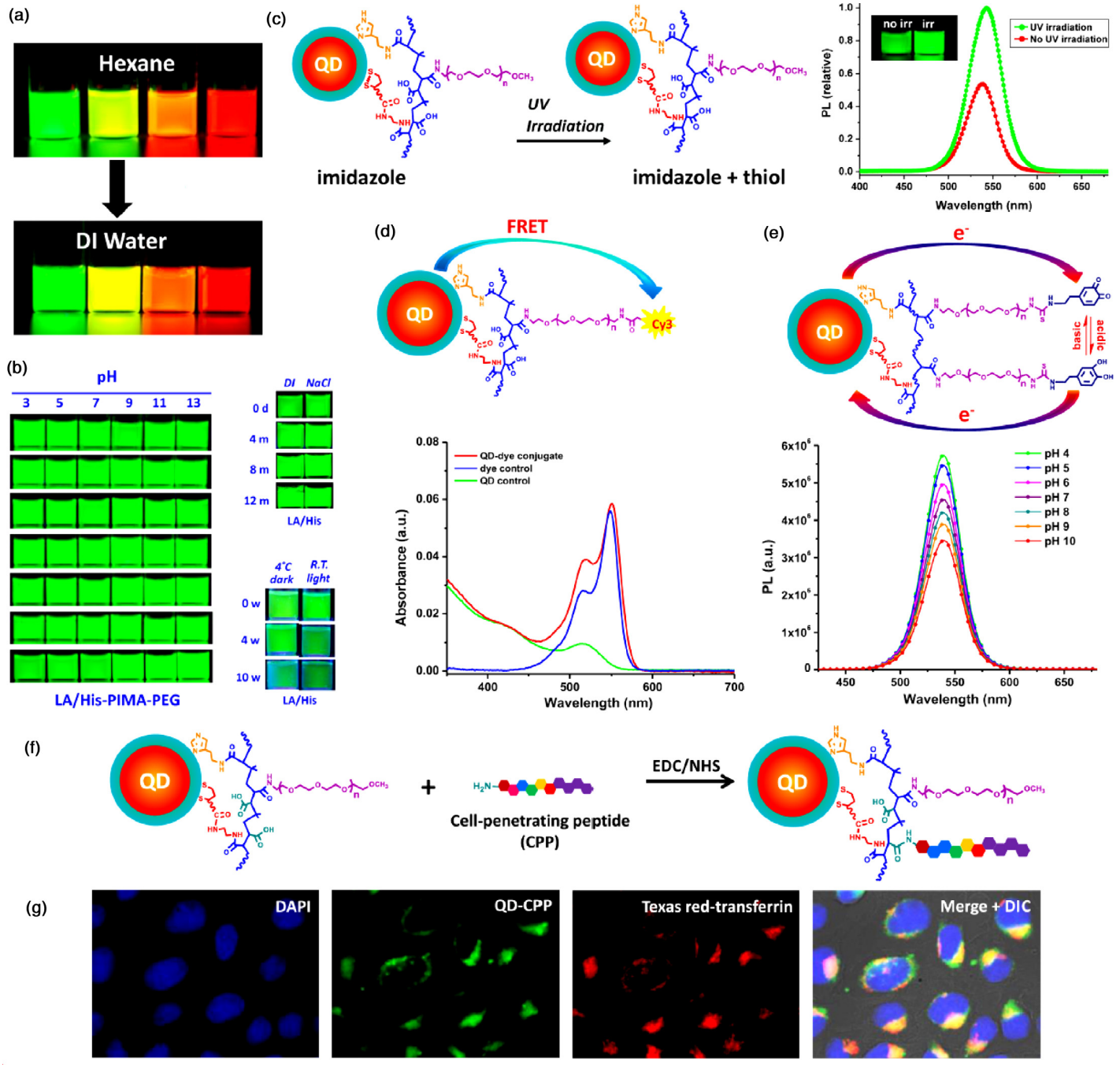


**FIGURE 13**

(A) Fluorescent photos of four sets of QDs capped with TOP/TOPO in hexane and LA/His-PIMA-PEG in water; (B) Fluorescent photos of long-term stability in a broad pH range (3–13), at 4 °C or under ambient conditions PL intensity and in the presence of excess electrolyte; (D) Schematic representation of the covalent conjugation of sulfo-Cy3 NHS-ester dye to amine-functionalized QDs with a FRET process; (E) Schematics of the assembly of dopamine-ITC onto amine-functionalized QDs via isothiourea bond with pH-controlled luminescence; (F) the QDCPP conjugate assembled via EDC/NHS coupling; (G) Representative epifluorescence images of HeLa cells incubated with QD-CPP conjugates at 200 nM for 1 h. Images correspond to the DAPI emission, QD emission at 537 nm, Texas Red-transferrin emission (as an endosome-specific marker), and the merged images. (Reprinted with permission from Ref. [111]. Copyright 2015 American Chemical Society).

(SWIR) QDs is burgeoning. Especially, SWIR-QDs will be more promising in the through-skull fluorescence imaging [117]. With the presented cross-sections of the chemo-/biological sensing that have been reported, the diversity of QDs in surface ligands-mediated applications will offer them with a promising future.

## Acknowledgments

This work was financially supported by the Open Project Program of State Key Laboratory of Organic-Inorganic Composites (oic-201701009), National Natural Science Foundation of China (Grant No. 21305066), Program for New Century Excellent Talents in University (NCET-12-0633) and the Jiangsu Province Natural Science Fund for Distinguished Young Scholars (BK20130032).

### References

[1] C.de.M. Donegá, Chem. Soc. Rev. 40 (3) (2011) 1512.
[2] U. Resch-Genger, et al. Nat. Methods 5 (9) (2008) 763.
[3] R. Freeman, et al. Chem. Soc. Rev. 41 (10) (2012) 4067.
[4] K.D. Wegner, et al. Chem. Soc. Rev. 44 (14) (2015) 4792.
[5] E. Petryayeva, et al. Appl. Spectrosc. 67 (3) (2013) 215.
[6] W.R. Algar, et al. Anal. Chem. 83 (23) (2011) 8826.
[7] M.A. Boles, et al. Nat. Mater. 15 (3) (2016) 364.
[8] M.D. Peterson, et al. Annu. Rev. Phys. Chem. 65 (2014) 317.
[9] D.V. Talapin, et al. Nano Lett. 1 (4) (2001) 209.
[10] A.M. Munro, et al. J. Phys. Chem. C 111 (17) (2007) 6220.
[11] S. Jeong, et al. J. Am. Chem. Soc. 127 (29) (2005) 10126.
[12] J. Huang, et al. J. Am. Chem. Soc. 132 (13) (2010) 4858.
[13] I.L. Medintz, et al. Nat. Mater. 2 (9) (2003) 630.
[14] J. Ostermann, et al. Beilstein J. Nanotechnol. 6 (2015) 232.
[15] S. Silv, et al. Chem. Soc. Rev. 44 (13) (2015) 4275.
[16] T. Mizuhara, et al. Nano Today 11 (1) (2016) 31.
[17] P. Reiss, et al. Chem. Rev. 116 (18) (2016) 10731.
[18] P.L. Saldanha, et al. Nano Today 12 (2017) 46.
[19] K.E. Sapsford, et al. Chem. Rev. 113 (3) (2013) 1904.
[20] J.B. Blanco-Canosac, et al. Coord. Chem. Rev. 263 (2014) 101.
[21] W.W. Yu, et al. Chem. Mater. 15 (22) (2003) 4300.
[22] A.J. Morris-Cohen, et al. J. Phys. Chem. Lett. 1 (7) (2010) 1078.
[23] Y. Gao, et al. J. Am. Chem. Soc. 136 (18) (2014) 6724.
[24] M. Green, J. Mater. Chem. 20 (28) (2010) 5797.
[25] D. Zhou, et al. Chem. Mater. 23 (21) (2011) 4857.
[26] C. Wang, et al. J. Mater. Chem. C 2 (4) (2014) 660.
[27] F. Dubois, et al. J. Am. Chem. Soc. 129 (3) (2007) 482.
[28] N. Zhan, et al. Nat. Protoc. 10 (2015) 859.
[29] A. Nag, et al. Z. Phys. Chem. 229 (1–2) (2015) 85.
[30] A. Nag, et al. J. Am. Chem. Soc. 133 (27) (2011) 10612.
[31] H. Zhang, et al. ACS Nano 8 (7) (2014) 7359.
[32] J. Huang, et al. ACS Nano 8 (9) (2014) 9388.
[33] J. Pichaandi, et al. Chem. Mater. 25 (10) (2013) 2035.
[34] C. Schieber, et al. Angew. Chem. Int. Ed. 51 (42) (2012) 10523.
[35] P. Zhang, et al. J. Am. Chem. Soc. 134 (20) (2012) 8388.
[36] Z. Hong, et al. ACS Nano 9 (12) (2015) 11750.
[37] N. Zhan, et al. J. Am. Chem. Soc. 138 (9) (2016) 3190.
[38] P.D. Howes, et al. Science 346 (6205) (2014).
[39] G.M. Durán, et al. Talanta 131 (2015) 286.
[40] J. Park, et al. ACS Nano 9 (6) (2015) 6511.
[41] C. Schmidtke, et al. Langmuir 29 (40) (2013) 12593.
[42] Y. Yang, et al. Acc. Chem. Res. 47 (7) (2014) 1950.
[43] J. Ma, et al. Chem. Eur. J. 22 (39) (2016) 13805.
[44] K.V. Joshi, et al. Analyst 137 (20) (2012) 4647.
[45] S. Manda, et al. J. Phys. Chem. C 117 (6) (2013) 3069.
[46] J. Zhou, et al. TrAC Trends Anal. Chem. 65 (2015) 22.
[47] J. Aguilera-Sigalat, et al. Chem. Commun. 48 (20) (2012) 2573.
[48] X. Ai, et al. Talanta 99 (2012) 409.
[49] M. Algarra, et al. Mater. Sci. Eng. C 32 (4) (2012) 799.
[50] Y. Cao, et al. J. Fluoresc. 25 (5) (2015) 1397.
[51] G.M. Durán, et al. Anal. Methods 7 (2015) 3472.
[52] X.-F. Chen, et al. Appl. Surf. Sci. 263 (2012) 491.
[53] Z. Zhang, et al. Nanoscale 7 (46) (2015) 19540.
[54] U. Tohgha, et al. ACS Nano 7 (12) (2013) 11094.
[55] Y. Cao, et al. J. Mol. Struct. 1031 (5) (2013) 9.
[56] Y. Wei, et al. Polym. Chem. 6 (4) (2015) 591.
[57] S.-Y. Liu, et al. Luminescence 31 (1) (2016) 96.
[58] R. Freeman, et al. Nano Lett. 9 (5) (2009) 2073.
[59] J. Zhou, et al. Nanoscale 8 (10) (2016) 5621.
[60] J. Zhang, et al. Nano Today 11 (3) (2016) 309.
[61] Y. Lou, et al. J. Mater. Chem. C 2 (2) (2014) 595.
[62] P. Wu, et al. Nanoscale 6 (1) (2014) 43.
[63] Q. Zhao, et al. J. Hazard. Mater. 250 (2013) 45.
[64] J. Ke, et al. Sci. Rep. 4 (2014) 5624.
[65] Y. Ding, et al. Sens. Actuators B-Chem. 203 (203) (2014) 35.
[66] D. Wu, et al. Sens. Actuators A-Phys. 205 (1) (2014) 72.
[67] C. Hao, et al. Biosens. Bioelectron. 36 (1) (2012) 174.
[68] D. Huang, et al. Anal. Chem. 85 (2) (2013) 1164.
[69] D. Huang, et al. Environ. Sci. Technol. 47 (9) (2013) 4392.
[70] T. Sung, et al. Sens. Actuators B-Chem. 165 (1) (2012) 119.
[71] X. Wang, et al. Talanta 84 (2) (2011) 382.
[72] L.H. Jin, et al. Anal. Chem. 86 (15) (2014) 7209.
[73] N. Butwong, et al. Spectrochim. Acta A-Mol. Biomol. Spectrosc. 97 (6) (2012) 17.
[74] W.E. Mahmoud, et al. Sens. Actuators B-Chem. 164 (1) (2012) 76.
[75] H.R. Rajabi, et al. Spectrochim. Acta A-Mol. Biomol. Spectrosc. 107 (7) (2013) 256.
[76] M. Shamsipur, et al. Mater. Sci. Eng. C 36 (1) (2014) 139.
[77] J. Sha, et al. Dyes Pigments 113 (2015) 102.
[78] J. Yao, et al. Anal. Chem. 85 (13) (2013) 6461.
[79] C. Yuan, et al. Anal. Chem. 84 (22) (2012) 9792.
[80] A. Jaiswal, et al. Langmuir 28 (44) (2012) 15687.
[81] D.M. Han, et al. Electrochem. Commun. 51 (2015) 72.
[82] I. Costas-Mora, et al. Anal. Chim. Acta 788 (2013) 114.
[83] I.C. Serrano, et al. RSC Adv. 3 (27) (2013) 10691.
[84] B. Ji, et al. Nat. Nanotechnol. 10 (2) (2015) 170.
[85] V.V. Goftman, et al. Biosens. Bioelectron. 79 (2016) 476.
[86] M.F. Foda, et al. ACS Appl. Mater. Interfaces 6 (3) (2014) 2011.
[87] Z. Lin, et al. New J. Chem. 38 (1) (2014) 90.
[88] B.-H. Jun, et al. Adv. Funct. Mater. 22 (9) (2012) 1843.
[89] S.A. Díaz, et al. ACS Nano 5 (4) (2011) 2795.
[90] C. Zhou, et al. J. Colloid Interface Sci. 478 (2016) 88.
[91] E.S. Speranskaya, et al. Biosens. Bioelectron. 53 (4) (2014) 225.
[92] C. Schmidtke, et al. Nanoscale 5 (16) (2013) 7433.
[93] C. Schmidtke, et al. J. Phys. Chem. C 117 (16) (2013) 8570.
[94] E. Pöselt, et al. ACS Nano 6 (4) (2012) 3346.
[95] J. Ostermann, et al. ACS Nano 7 (10) (2013) 9156.
[96] N.V. Beloglazova, et al. J. Mater. Chem. B 3 (2) (2015) 180.
[97] O. Carion, et al. Nat. Protoc. 2 (10) (2007) 2383.
[98] S. Tong, et al. Nano Lett. 11 (9) (2011) 3720.
[99] W. Zheng, et al. J. Am. Chem. Soc. 136 (5) (2014) 1992.
[100] R. Hu, et al. Theranostics 2 (7) (2012) 723.
[101] S. Taniguchi, et al. ACS Appl. Mater. Interfaces 8 (7) (2016) 4887.
[102] K. Susumu, et al. J. Am. Chem. Soc. 129 (45) (2007) 13987.
[103] E. Gravel, et al. Chem. Sci. 4 (1) (2013) 411.
[104] J. Park, et al. Adv. Funct. Mater. 21 (2011) 1558.
[105] K. Susumu, et al. J. Am. Chem. Soc. 133 (24) (2011) 9480.
[106] E. Muro, et al. J. Am. Chem. Soc. 132 (13) (2010) 4556.
[107] N. Zhan, et al. ACS Appl. Mater. Interfaces 5 (8) (2013) 2861.
[108] N. Zhan, et al. J. Am. Chem. Soc. 135 (37) (2013) 13786.
[109] K. Susumu, et al. Chem. Mater. 26 (18) (2014) 5327.
[110] A.M. Smith, et al. J. Am. Chem. Soc. 130 (34) (2008) 11278.
[111] W. Wang, et al. J. Am. Chem. Soc. 137 (16) (2015) 5438.
[112] L. Ma, et al. J. Am. Chem. Soc. 138 (10) (2016) 3382.
[113] E. Giovanelli, et al. Langmuir 28 (43) (2012) 15177.
[114] R. Kubotaa, et al. Chem. Soc. Rev. 44 (13) (2015) 4454.
[115] G. Xu, et al. Chem. Rev. 116 (19) (2016) 12234.
[116] D. Franke, Nat. Commun. 7 (2016) 12749.
[117] E. Oh, Nat. Nanotechnol. 11 (2016) 479.